

Ordered Mesoporous Pd/Silica–Carbon as a Highly Active Heterogeneous Catalyst for Coupling Reaction of Chlorobenzene in Aqueous Media

Ying Wan,^{*,†} Haiyan Wang,[†] Qingfei Zhao,[†] Miia Klingstedt,[‡] Osamu Terasaki,[‡] and Dongyuan Zhao[§]

Department of Chemistry, Shanghai Normal University, Shanghai 200234, People's Republic of China, Arrhenius Laboratory, Department of Physical, Inorganic and Structural Chemistry, Stockholm University, Stockholm 10691, Sweden, and Department of Chemistry and Shanghai Key Laboratory of Molecular Catalysis and Innovative Materials, Fudan University, Shanghai 200433, People's Republic of China

Received November 5, 2008; E-mail: ywan@shnu.edu.cn

Abstract: Heterogeneous palladium catalysts, which are supported on ordered mesoporous silica–carbon nanocomposites, have been applied in water-mediated coupling reactions of chlorobenzene without assistance of any phase-transfer catalysts. Characterization by XRD, TEM, N₂ sorption, FT-IR, TG, XPS, and H₂ chemisorption techniques reveals the highly ordered mesostructure, high surface areas (~345 m²/g), large pore volumes (~0.46 cm³/g), uniform mesopore sizes (~6.3 nm), hybrid silicate and carbonaceous compositions, and a high dispersion of palladium nanoparticles (about 3 nm) in the mesopores. The catalyst exhibits a high yield for *trans*-stilbene (~60%) in the Heck coupling reaction of chlorobenzene and styrene at 100 °C and for biphenyl (46%) in the Ullmann coupling reaction of chlorobenzene at 30 °C, using water as a solvent. When substituted aryl chlorides (hydroxyl, methoxyl, and methyl) are involved in the Ullmann reaction, the yields of symmetrical substituted biphenyl are also higher than 44% (this value reaches 86% for the coupling reaction of 4-chlorophenol) at a low temperature of 30 °C. This heterogeneous catalyst is stable, which shows negligible metal leaching, and can be reused more than 20 times. For comparison, the catalytic activities for Pd catalysts supported on pure mesoporous polymeric, carbonaceous, and silicate frameworks are also investigated. The results clearly indicate that the pore wall nature shows great influence on the dispersion of metallic Pd species and, in turn, the catalytic performance.

1. Introduction

Hybrid mesoporous nanocomposites have received much attention during recent years because of the combination of their multifunctionality, for example, unique properties unachievable in traditional materials, with well-controlled pore structures, high surface areas, and large and tunable pore sizes which facilitate the diffusion of reactant and product inside the pores.^{1–15} Mesoporous carbon-based nanocomposites are, in particular,

interesting owing to the potential applications as catalyst supports, adsorbents, electrodes, etc.^{11–15} In industry, supported palladium/carbon are frequently used heterogeneous catalysts in hydrogenation and coupling reactions.^{16–18} Traditionally used activated carbon-based materials have broad pore size distributions, ranging from micropores to macropores. This phenomenon may lead to a nonuniform distribution of metal active sites, limit their applications, and fail to establish the relationship between pore texture/surface nature/metal size of catalysts and catalytic performance.¹⁹ On comparison with traditional activated carbon carriers, mesoporous carbons have advantages in tuning pore structure, pore size, and pore surface chemistry and, hence, may

[†] Shanghai Normal University.

[‡] Stockholm University.

[§] Fudan University.

- (1) Sayari, A.; Hamoudi, S. *Chem. Mater.* **2001**, *13*, 3151.
- (2) Innocenzi, P.; Brusatin, G. *Chem. Mater.* **2001**, *13*, 3126.
- (3) Sayen, S.; Etienne, M.; Bessiere, J.; Walcarius, A. *Electroanalysis* **2002**, *14*, 1521.
- (4) Pang, J. B.; John, V. T.; Loy, D. A.; Yang, Z. Z.; Lu, Y. F. *Adv. Mater.* **2005**, *17*, 704.
- (5) Pardo, E.; Burguete, P.; Ruiz-Garcia, R.; Julve, M.; Beltran, D.; Journaux, Y.; Amoros, P.; Lloret, F. *J. Mater. Chem.* **2006**, *16*, 2702.
- (6) Angloher, S.; Kecht, J.; Bein, T. *Chem. Mater.* **2007**, *19*, 5797.
- (7) Wei, Y.; Jin, D. L.; Yang, C. C.; Kels, M. C.; Qiu, K. Y. *Mater. Sci. Eng., C* **1998**, *6*, 91.
- (8) Asefa, T.; MacLachan, M. J.; Coombs, N.; Ozin, G. A. *Nature* **1999**, *402*, 867.
- (9) Inagaki, S.; Guan, S.; Fukushima, Y.; Ohsuna, T.; Terasaki, O. *J. Am. Chem. Soc.* **1999**, *121*, 9611.
- (10) Anderson, M. L.; Stroud, R. M.; Rolison, D. R. *Nano Lett.* **2002**, *2*, 235.

- (11) Scott, B. J.; Wirnsberger, G.; Stucky, G. D. *Chem. Mater.* **2001**, *13*, 3140.
- (12) Choi, M.; Kleitz, F.; Liu, D. N.; Lee, H. Y.; Ahn, W. S.; Ryoo, R. *J. Am. Chem. Soc.* **2005**, *127*, 1924.
- (13) Mastai, Y.; Polarz, S.; Antonietti, M. *Adv. Funct. Mater.* **2002**, *12*, 197.
- (14) Tsionsky, M.; Gun, G.; Glezer, V.; Lev, O. *Anal. Chem.* **1994**, *66*, 1747.
- (15) Liu, R. L.; Shi, Y. F.; Wan, Y.; Meng, Y.; Zhang, F. Q.; Gu, D.; Chen, Z. X.; Tu, B.; Zhao, D. Y. *J. Am. Chem. Soc.* **2006**, *128*, 11652.
- (16) Balachari, D.; Quinn, L.; O'Doherty, G. A. *Tetrahedron Lett.* **1999**, *40*, 4769.
- (17) Kohler, K.; Heidenreich, R. G.; Krauter, J. G. E.; Pietsch, M. *Chem.–Eur. J.* **2002**, *8*, 622.
- (18) Yin, L. X.; Liebscher, J. *Chem. Rev.* **2007**, *107*, 133.
- (19) Kyotani, T. *Carbon* **2000**, *38*, 269.

enhance the catalytic activity.^{20–25} However, ordered mesoporous carbon-based nanocomposites are difficult to obtain. Direct carbonization of organic–inorganic frameworks (or two phases) or adding carbon particles to silica networks can yield mesoporous silica–carbon nanocomposites.^{4,9} Random distribution of two constituents, pore blockage, phase separation, disordered structure, or uneconomic processes are the problems.^{26,27} The postsynthesis for the mesoporous carbon-based materials always undergoes rigorous conditions, leading to the destruction of the mesostructure.^{28,29} Recently, several groups reported the surfactant self-assembly approach to synthesize mesoporous carbon and carbon-based nanocomposites.^{15,30–34} By using cheap, soluble phenolic resins as carbon precursors, TEOS as a silica precursor, and commercially available triblock copolymer as a structure-directing agent, highly ordered hybrid mesoporous silica–carbon nanocomposites with tunable pore sizes can be produced in batch.¹⁵ Up to now, there have been no studies published on the catalytic behaviors of mesoporous carbon and silica–carbon nanocomposites derived from the surfactant self-assembly. The application of hybrid silica–carbon as metallic catalyst carriers would pave the way for further tailoring and understanding the role of nanophases for bulk properties.

Carbon–carbon (C–C) coupling reactions, such as Ullmann and Heck reactions, have profound importance for applications in chemical, pharmaceutical, and biochemical industries.^{35–50}

Although homogeneous catalysts have been extensively investigated for these reactions, they suffer from the difficult separation with reaction media, nonreusability, and deactivation due to the aggregation of metallic particles during the reactions.^{38,39} Recycling of catalysts is a task of great economic and environmental importance in the industry.⁴⁰ In this context, heterogeneous catalysts are desired because of easy separation, recycling, and the use of a small amount in the production. The search for new efficient and recyclable heterogeneous catalysts has, therefore, received more and more attention. The Pd/activated carbon (AC) and mesoporous silica catalysts have been used to replace conventional homogeneous catalyst for the Ullmann and Heck coupling reactions. Mehnert et al.⁴¹ grafted Pd complex onto an alkylating Nb-MCM-41. The catalyst showed a good activity in the Heck coupling reaction of arylbromide with styrene. Yang et al.⁴² found that the immobilization of Pd ions onto the dicyano-functionalized MCM-41 improved the Heck reaction. However, the reactions are usually carried out under rigorous conditions, for example, high temperature (sometimes autoclave for Heck coupling) and the presence of an organic solvent such as *N,N*-dimethylformate (DMF),⁴³ *N*-methylpyrrolidone,^{44,45} or toluene^{46–48} and phase-transfer catalyst such as crown ether,³⁵ polyethylene glycol,⁴⁹ tetrabutylammonium chloride,⁵⁰ etc. From the viewpoint of the environmentally benign organic reactions, water-containing media are popular due to reduction of burden for organic solvent disposal.^{51–54} In this case, a highly efficient catalyst which can adsorb and activate substrate is of great significance.⁵⁵ Very recently, we found that Pd/phenyl group functionalized mesoporous silica shows a better catalytic performance on converting iodo- and bromobenzene to biphenyl from the Ullmann coupling reaction than Pd/AC.^{56,57} The hybrid inorganic–organic nature and uniform mesopores of the mesoporous carrier are possibly responsible for the improvement.^{56–59} However, mesoporous silica always undergoes the problem with instability in hot water. Long-time run would lead to mesostructure destruction. The recycling of mesoporous silica-based catalysts in the coupling reactions in most cases, especially when water is involved, is less than 10 times. On the other hand, aryl bromides and aryl iodides are always the reactants, and low activities were observed for aryl chlorides. Aryl chlorides are cheaper and more common than aryl bromides and aryl iodides, being more valuable in the coupling reaction. More distinctly, Cl-containing organic compounds are one of the most serious contaminants in water.^{60–62} The coupling reaction or the dehydrochlorination

- (20) Ryoo, R.; Joo, S. H.; Kruk, M.; Jaroniec, M. *Adv. Mater.* **2001**, *13*, 677.
- (21) Yang, H. F.; Zhao, D. Y. *J. Mater. Chem.* **2005**, *15*, 1217.
- (22) Lu, A. H.; Schuth, F. *Adv. Mater.* **2006**, *18*, 1793.
- (23) Lee, J.; Kim, J.; Hyeon, T. *Adv. Mater.* **2006**, *18*, 2073.
- (24) Ryoo, R.; Joo, S. H.; Jun, S. J. *Phys. Chem. B* **1999**, *103*, 7743.
- (25) Tiemann, M. *Chem. Mater.* **2008**, *20*, 961.
- (26) Wang, Z. M.; Hohsinoo, K.; Shishibori, K.; Kanoh, H.; Ooi, K. *Chem. Mater.* **2003**, *15*, 2926.
- (27) Lee, J.; Kim, J.; Lee, Y.; Yoon, S.; Oh, S. M.; Hyeon, T. *Chem. Mater.* **2004**, *16*, 3323.
- (28) Li, Z. J.; Del Cul, G. D.; Yan, W. F.; Liang, C. D.; Dai, S. J. *Am. Chem. Soc.* **2004**, *126*, 12782.
- (29) Li, Z. J.; Dai, S. *Chem. Mater.* **2005**, *17*, 1717.
- (30) Liang, C. D.; Hong, K. L.; Guiochon, G. A.; Mays, J. W.; Dai, S. *Angew. Chem., Int. Ed.* **2004**, *43*, 5785.
- (31) Tanaka, S.; Nishiyama, N.; Egashira, Y.; Ueyama, K. *Chem. Commun.* **2005**, 2125.
- (32) Meng, Y.; Gu, D.; Zhang, F. Q.; Shi, Y. F.; Yang, H. F.; Li, Z.; Yu, C. Z.; Tu, B.; Zhao, D. Y. *Angew. Chem., Int. Ed.* **2005**, *44*, 7053.
- (33) Wan, Y.; Qian, X.; Jia, N. Q.; Wang, Z. Y.; Li, H. X.; Zhao, D. Y. *Chem. Mater.* **2008**, *20*, 1012.
- (34) Wan, Y.; Shi, Y. F.; Zhao, D. Y. *Chem. Mater.* **2008**, *20*, 932.
- (35) Venkatraman, S.; Li, C. J. *Org. Lett.* **1999**, *1*, 1133.
- (36) Mukhopadhyay, S.; Rothenberg, G.; Gitis, D.; Sasson, Y. *Org. Lett.* **2000**, *2*, 211.
- (37) Hassan, J.; Sevignon, M.; Gozzi, C.; Schulz, E.; Lemaire, M. *Chem. Rev.* **2002**, *102*, 1359.
- (38) Zhao, F. Y.; Bhanage, B. M.; Shirai, M.; Arai, M. *J. Mol. Catal. A* **1999**, *142*, 383.
- (39) Reetz, M. T.; de Vries, J. G. *Chem. Commun.* **2004**, 1559.
- (40) Cole-Hamilton, D. J. *Science* **2003**, *299*, 1702.
- (41) Mehnert, C. P.; Weaver, D. W.; Ying, J. Y. *J. Am. Chem. Soc.* **1998**, *120*, 12289.
- (42) Yang, H. Q.; Zhang, G. Y.; Hong, X. L.; Zhu, Y. Y. *J. Mol. Catal. A* **2004**, *210*, 143.
- (43) Stevens, P. D.; Li, G. F.; Fan, J. D.; Yen, M.; Gao, Y. *Chem. Commun.* **2005**, 4435.
- (44) Seki, M. *Synthesis* **2006**, 2975.
- (45) Zhao, F. Y.; Bhanage, B. M.; Shirai, M.; Arai, M. *Chem.—Eur. J.* **2000**, *6*, 843.
- (46) Hallberg, A.; Westfelt, L. *J. Chem. Soc., Perkin Trans. 1* **1984**, 933.
- (47) Andersson, C. M.; Hallberg, A.; Daves, G. D. *J. Org. Chem.* **1987**, *52*, 3529.
- (48) Andersson, C. M.; Hallberg, A. *J. Org. Chem.* **1988**, *53*, 235.
- (49) Mukhopadhyay, S.; Rothenberg, G.; Gitis, D.; Wiener, H.; Sasson, Y. *J. Chem. Soc., Perkin Trans. 2* **1999**, 2481.
- (50) Papp, A.; Galbacs, G.; Molnar, R. *Tetrahedron Lett.* **2005**, *46*, 7725.

- (51) Li, C. J. *Chem. Rev.* **2005**, *105*, 3095.
- (52) Wu, X. F.; Liu, J. K.; Li, X. H.; Zanotti-Gerosa, A.; Hancock, F.; Vinci, D.; Ruan, J. W.; Xiao, J. L. *Angew. Chem., Int. Ed.* **2006**, *45*, 6718.
- (53) Narayan, S.; Muldoon, J.; Finn, M. G.; Fokin, V. V.; Kolb, H. C.; Sharpless, K. B. *Angew. Chem., Int. Ed.* **2005**, *44*, 3275.
- (54) Wu, X. F.; Li, X. H.; Zanotti-Gerosa, A.; Pettman, A.; Liu, J. K.; Mills, A. J.; Xiao, J. L. *Chem.—Eur. J.* **2008**, *14*, 2209.
- (55) Wight, A. P.; Davis, M. E. *Chem. Rev.* **2002**, *102*, 3589.
- (56) Wan, Y.; Chen, J.; Zhang, D. Q.; Li, H. X. *J. Mol. Catal. A* **2006**, *258*, 89.
- (57) Wan, Y.; Zhang, D. Q.; Zhai, Y. P.; Feng, C. M.; Chen, J.; Li, H. X. *Chem. Asian J.* **2007**, *2*, 875.
- (58) Li, H. X.; Chen, J.; Wan, Y.; Chai, W.; Zhang, F.; Lu, Y. F. *Green Chem.* **2007**, *9*, 273.
- (59) Li, H. X.; Chai, W.; Zhang, F.; Chen, J. *Green Chem.* **2007**, *9*, 1223.
- (60) Squillace, P. J.; Moran, M. J.; Lapham, W. W.; Price, C. V.; Clawges, R. M.; Zogorski, J. S. *Environ. Sci. Technol.* **1999**, *33*, 4176.
- (61) Fritsch, D.; Kuhr, K.; Mackenzie, K.; Kopinke, F. D. *Catal. Today* **2003**, *82*, 105.
- (62) Vogt, C.; Alfreider, A.; Lorbeer, H.; Hoffmann, D.; Wuensche, L.; Babel, W. *J. Contam. Hydrol.* **2004**, *68*, 121.

is difficult due to the high energy of C–Cl bonds.^{63,64} Therefore, developing new catalysts that can activate aryl chlorides and allow the coupling reactions of aryl chlorides occurring in aqueous media is important.

Here we report the water-mediated coupling reactions of aryl chlorides over heterogeneous palladium catalysts, which are supported on ordered mesoporous silica–carbon nanocomposites. The mesoporous nanocomposites are produced on the basis of a triblock copolymer templating approach, possessing large pore sizes and hybrid pore surface constituted by carbon and silica. The latter feature supports a high dispersion of palladium nanoparticles (~3 nm). The novel Pd catalyst exhibits an impressive yield close to 60% for *trans*-stilbene at a low temperature of 100 °C in Heck coupling of chlorobenzene and styrene and a yield of 46% for biphenyl at 30 °C in Ullmann coupling of chlorobenzene. When substituted aryl chlorides (such as –OH, –OCH₃, and –CH₃) are involved in the system, the yield of symmetrical substituted biphenyl is also higher than 44% (this value reaches 86% for the coupling reaction of 4-chlorophenol) at 30 °C. The catalytic coupling reactions are of great significance owing to the use of water as a clean and environmentally benign solvent and aryl chlorides as reactants. The heterogeneous catalyst Pd/MSC is stable, which shows negligible metal leaching and can be reused more than 20 times. To understand the effect of pore wall compositions on the metal distribution and hence the catalytic performance, the growth of Pd particles in the mesochannels of mesoporous polymer, carbon, and silica and their catalytic performance are also investigated. The pore wall nature and porosity show great influence on the dispersion of active Pd sites and the production of *trans*-stilbene or biphenyl.

2. Experimental Section

2.1. Catalyst Preparation. The ordered mesoporous silica–carbon composite (MSC) supports were synthesized via a surfactant-templating method by using soluble phenolic resins and tetraethyl orthosilicate (TEOS) as carbon and silica precursors and the triblock copolymer F127 as a structure-directing agent.¹⁵ For comparison, mesoporous polymers (MP), carbons (MC), and silicas (MS) were also prepared according to the established procedures.^{32,65} Soluble phenolic resins were prepared by the base-catalyzed polymerization of phenol and formaldehyde.³² The phenolic resin and F127 were dissolved in ethanol with a mass composition of phenol/HCHO/F127 = 0.61:0.39:1.0. Then the solution was poured into several dishes. After ethanol evaporation at room temperature for 8 h and thermopolymerization at 100 °C for 24 h, the membranes peeled off from the dishes. The as-made samples were then heated at 350 °C for 4 h under nitrogen to obtain MP. MC was a product after further carbonization at 900 °C for 4 h. When the initial solution contained phenolic resin, TEOS, triblock copolymer F127, 0.2 M HCl, and ethanol with the mass ratio of phenol/HCHO/TEOS/HCl/F127 = 0.61:0.39:2.08:1.0:1.6, the black powders after the above carbonization (MSC) were composed of silica and carbon. Pure mesoporous silica MS was synthesized by the hydrothermal method in which the initial solutions contained 2.08 g of TEOS, 1.0 g of P123, 30 g of 2 M HCl, and 7.5 g of H₂O. The hydrothermal temperature and time was 100 °C and 24 h. After surfactant removal at 550 °C under air, the MS carrier was obtained.

Supported palladium catalysts were prepared by isochoric impregnation. In a typical procedure, 0.8 g of an aqueous solution

of PdCl₂ (1.1 wt %) were impregnated with 0.1 g of dry MSC carrier. The mixture was placed in a hood overnight. Then the catalysts were dried at 100 °C, reduced at 200 °C in forming gas (10 vol % H₂ in nitrogen) for 3 h, and named as fresh supported catalysts (Pd/MSC, Pd/MP, Pd/MC, and Pd/MS).

2.2. Characterization. The X-ray diffraction (XRD) measurements were taken on a Rigaku Dmax-3C diffractometer using Cu K α radiation (40 kV, 30 mA, $\lambda = 0.15408$ nm). The *d* spacing values were calculated by the formula $d = \lambda/2\sin \theta$, and the unit cell parameters were calculated from the formula $a_0 = 2d_{100}/\sqrt{3}$. The metallic Pd sizes were estimated according to the Scherrer formula: $\text{size} = 0.89\lambda/\beta\cos \theta$ on the basis of the 111 diffraction peak in wide-angle XRD patterns. N₂ adsorption–desorption isotherms were measured at 77 K with a Quantachrome NOVA 4000e analyzer. The Brunauer–Emmett–Teller (BET) method was utilized to calculate the specific surface areas (S_{BET}). By using the Barrett–Joyner–Halenda (BJH) model, the pore volumes and pore size distributions were derived from the adsorption branches of isotherms. The micropore surface area ($S_{\text{BET}}^{\text{micro}}$) was calculated from the *V*–*t* plot method. A JEM 2100F microscope, equipped with a field emission gun, operated at 200 kV was used for the scanning transmission electron microscopy-high angle annular dark field (STEM-HAADF) imaging. With a probe size of 0.2 nm, inner and outer semiangles for the HAADF detector were 76 and 203 mrad, respectively. Transmission electron microscopy (TEM) experiments were conducted using a JEM 2100 microscope operated at 200 kV. Energy dispersive X-ray spectroscopy (EDX) was performed on a Philips EDAX instrument. Fourier transform infrared (FT-IR) spectra were collected on a Nicolet Fourier spectrophotometer, using KBr pellets of the solid samples. The C, H, and O content was measured on a Vario EL III elemental analyzer (Germany). Thermal gravity analysis (TG) curves were monitored on a Mettler Toledo 851e apparatus. X-ray photoelectron spectroscopy (XPS) measurements were performed on a Perkin-Elmer PHI 5000CESCA system with a base pressure of 10^{–9} Torr. The Pd loading on the carriers was determined by inductively coupled plasma-atomic emission spectrometry (ICP-AES, Varian VISTA-MPX). H₂ chemisorption was conducted on a Quantachrome CHEMBET-3000 system by pulsing hydrogen on the supported Pd catalyst. Palladium surface areas were calculated from H₂ chemisorption data assuming that all palladium particles were spherical and that the adsorption stoichiometry was one H atom per Pd metal.⁶⁶ The metal surface area (S_{Pd}) is given by the formula $S_{\text{Pd}} = 18.5V_{\text{ads}}N_0/22.4 \times 10^{20} \times \text{metal content (wt \%)}$ (here, the value of 18.5 is the surface area of one molecule of H₂ and V_{ads} is the volume of H₂ chemisorbed). The palladium size was estimated according to the formula $d = 5/\rho_{\text{Pd}}S_{\text{Pd}}$.

2.3. Catalytic Reactions. The coupling reactions were carried out in a 50 mL round-bottled flask with refluxing by using water as the solvent. The products were quantified by GC–mass analysis (Agilent 6890n-5973i equipped with a JW DB-5, 95% dimethyl 1-(5%)-diphenylpolysiloxane capillary column). The analysis was repeated at least three times for all tests, and the experimental errors were within $\pm 5\%$. The products of the Heck coupling reaction have also been isolated and purified by column chromatography. The identification was conducted by ¹H NMR measurement on a Bruker DRX 400 spectrometer, using tetramethylsilane as the internal standard.

Heck coupling reactions. Typically, 0.80 g (7.5 mmol) of sodium carbonate (Na₂CO₃) was dissolved in 10 mL of water and placed in the reactor. To this were added 0.10 g (containing 0.047 mmol metallic Pd) of supported palladium catalyst and 0.55 g (5.0 mmol) of chlorobenzene, and the mixture was heated to 100 °C. Finally, 0.78 g (7.5 mmol) of styrene was added to start the coupling reaction. After 24 h stirring, the products were centrifuged, extracted with toluene, and analyzed. To study the leaching of Pd during the

(63) Grushin, V. V.; Alper, H. *Chem. Rev.* **1994**, *94*, 1047.

(64) Hassan, J.; Hathroubi, C.; Gozzi, C.; Lemaire, M. *Tetrahedron* **2001**, *57*, 7845.

(65) Zhao, D. Y.; Huo, Q. S.; Feng, J. L.; Chmelka, B. F.; Stucky, G. D. *J. Am. Chem. Soc.* **1998**, *120*, 6024.

(66) Wang, S. Y.; Moon, S. H.; Vannice, M. A. *J. Catal.* **1981**, *71*, 167.

reaction, hot filtration was also adopted.^{67,68} After reaction, 2.5 mL of water was added, and the mixture was hot filtered under vacuum. The solid was washed with water (2.5 mL) and toluene (5.0 mL), and the liquid phase was analyzed by ICP-AES and extracted with toluene to analyze the conversion and selectivity.

For kinetics study, 1.6 g (15 mmol) of Na_2CO_3 was dissolved in 20 mL of water and placed in the reactor. To this were added 0.20 g (containing 0.094 mmol metallic Pd) of supported palladium catalyst and 1.1 g (10 mmol) of chlorobenzene, and the mixture was heated to 100 °C. Finally, 1.56 g (15 mmol) of styrene was added to start the coupling reaction. We followed the course of the reaction by taking aliquots (50 μL) periodically, cooling them in an ice bath, centrifuging, and extracting with toluene (0.5 mL).

For the recycling study, Heck reaction was performed with chlorobenzene and styrene maintaining the same reaction conditions as described above, except using the recovered catalyst. Each time, after the completion of reaction, the catalyst was recovered by centrifugation and then washed thoroughly with toluene followed by a copious amount of water to remove the base present in the used catalyst. The recovered catalyst was dried under vacuum at 100 °C overnight, weighed, and reused in a next run. After the 21st run, hot filtration was adopted to determine the Pd leaching and chlorobenzene conversion. The palladium content of the solid was measured in the first and the last reuses. The catalyst after 15 runs was characterized, denoted as Pd/MS-15run.

For Ullmann coupling reactions, typically, 1.1 g (10 mmol) of aryl chloride, 10 mL of water, 2.2 g (21 mmol) of sodium formate, 2.8 g (50 mmol) of potassium hydroxide, and 0.10 g (containing 0.047 mmol metallic Pd) of supported palladium catalyst were charged to the vessel. The reaction temperature was adjusted between 30 and 100 °C. After 6 h stirring, the products were centrifuged, extracted with toluene, and analyzed by GC–mass analysis. In a separated reaction, a mixture containing methanol and water ($v/v = 1:1$) was used as a solvent.

3. Results and Discussion

3.1. Mesostructure and Chemical Compositions of Supported Palladium Catalysts. The syntheses of mesoporous carriers were on the basis of a supramolecular self-assembling approach using triblock copolymer F127 as a structure-directing agent.^{15,33} The hybrid mesoporous silica–carbon (MSC) carrier was prepared using phenolic resin as a carbon precursor and TEOS as a silica precursor, and the heating temperature was 900 °C. Mesoporous polymer (MP) and carbon (MC) carriers were successively obtained from the pure phenolic resin solution after heating at 350 and 900 °C. By using TEOS as the precursor, mesoporous silica (MS) was synthesized. The FT-IR spectrum (Figure 1) for MP shows the carbon–carbon bond stretching of 1,2,4- and 1,2,6-trisubstituted and phenyl alkyl ether-type substituted aromatic ring structures (1610 cm^{-1}) and vibration of tetrasubstituted benzene rings (1730 cm^{-1}), indicating the polymeric composition of MP. The elemental analysis reveals a C/H/O ratio of 7:5:1, confirming the polymer framework and the presence of plenty of oxygen-containing groups. The absence of these vibrations for MC implies the conversion from polymeric to carbonaceous framework. A strong vibration at about 1080 cm^{-1} for the Si–O bond confirms the silicate framework of mesoporous silica (MS). The presence of the above vibration in the FT-IR spectrum of MSC implies that the composite contains silica. The TG analyses show that the MP and MC supports can completely burn off between 300 and 700 °C (Supporting Information Figure S1), indicating that these materials are constituted of polymer or carbon. On the

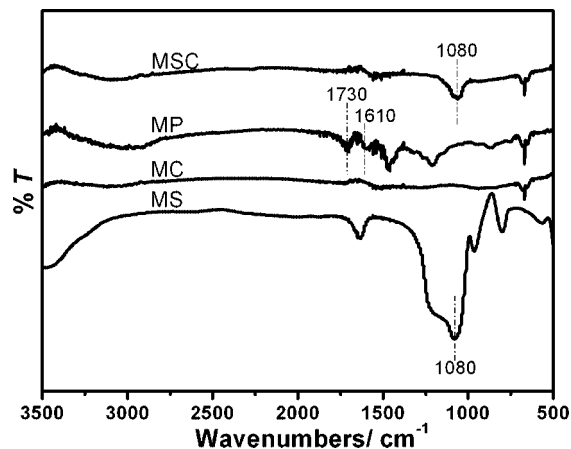


Figure 1. FT-IR spectra of mesoporous silica–carbon (MSC), polymer (MP), carbon (MC), and silica (MS) carriers.

contrary, no distinct weight loss is detected in this temperature range for MS, suggesting the composition of silica. MSC possesses a weight loss of 42% and a weight residue of 52%, implying that the carrier is composed of silica and carbon composites with the weight ratio of about 1.2:1. Supported palladium catalysts were prepared by isochoric impregnation of the supports with an aqueous solution of PdCl_2 and subsequent reduction. The palladium content for all catalysts is about 5 wt %, measured by ICP-AES.

All mesoporous carriers and supported palladium catalysts exhibit representative small-angle XRD patterns of the two-dimensional (2-D) hexagonal mesostructure (Figure 2), namely, one strong 10 diffraction at $2\theta = 0.5\text{--}1.5^\circ$ and two weak peaks (11 and 20) at higher angles. The cell parameters for the supported palladium catalysts are slightly lower than the values of the mesoporous carriers, implying the incorporation of Pd inside the mesochannels.⁶⁹ These results clearly indicate that the mesoporous silica–carbon composite, polymer, carbon, and silica carriers are stable, and the highly ordered mesostructure is retained after the impregnation of metallic solution, drying, and reduction. It should be noted that the diffraction peak intensity for Pd/MP is relatively weaker than that for the MP support, and the 11 diffraction disappears. The sorption isotherms of the catalysts show typical IV curves with significant nitrogen uptake under the relative pressures of 0.4–0.8 (Figure 3), indicative of uniform mesopores with the size ranging from 3 to 7 nm. The BET surface areas are higher than 340 m^2/g (Table 1). On comparison of the isotherms with mesoporous carriers (Supporting Information Figure S2), the incorporation of Pd shows minor effects on the pore size, pore volume, and surface area.

3.2. Growth of Metallic Palladium in Mesochannels. The metal dispersion in the heterogeneous catalyst is of great significance for the catalytic performance. Here the metal dispersion was investigated on the basis of mesoporous carriers with different framework compositions. The wide-angle XRD patterns for fresh Pd/MC and Pd/MSC after reduction in forming gas (Figure 4) show two broad reflections at 2θ of ~ 23 and 43° , which can be assigned to amorphous carbon for fresh mesoporous carbon-supported catalysts. Pd/MS shows one broad reflection at about 23° in the XRD pattern, corresponding to amorphous silica, and Pd/MP displays one broad reflection at

(67) Corma, A.; Das, D.; Garcia, H.; Leyva, A. *J. Catal.* **2005**, *229*, 322.

(68) Polshettiwar, V.; Molnar, A. *Tetrahedron* **2007**, *63*, 6949.

(69) Sakamoto, Y.; Fukuoka, A.; Higuchi, T.; Shimomura, N.; Inagaki, S.; Ichikawa, M. *J. Phys. Chem. B* **2004**, *108*, 853.

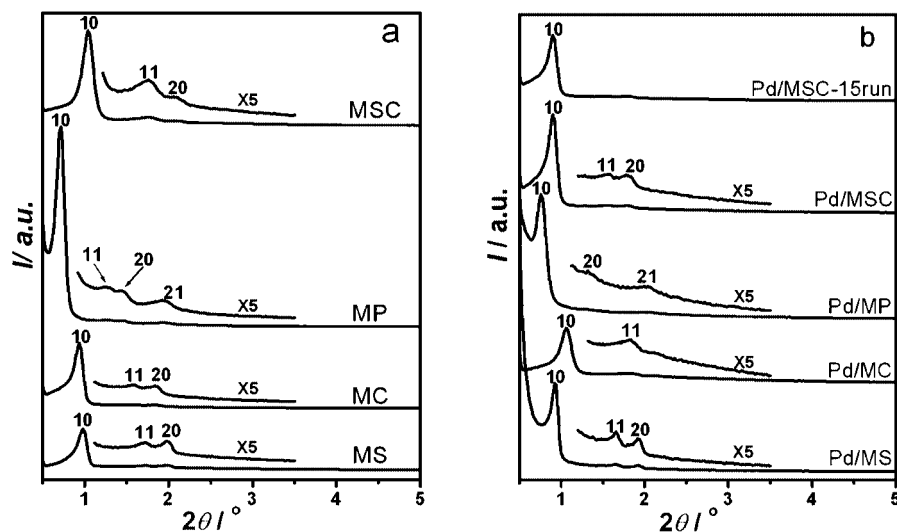


Figure 2. Small-angle XRD patterns of the mesoporous silica–carbon (MSC), polymer (MP), carbon (MC), and silica (MS) carriers (a), fresh and spent mesoporous supported palladium catalysts (b). Pd/MSC-15run in (b) denotes the heterogeneous palladium catalyst after 15 catalytic Heck reaction runs.

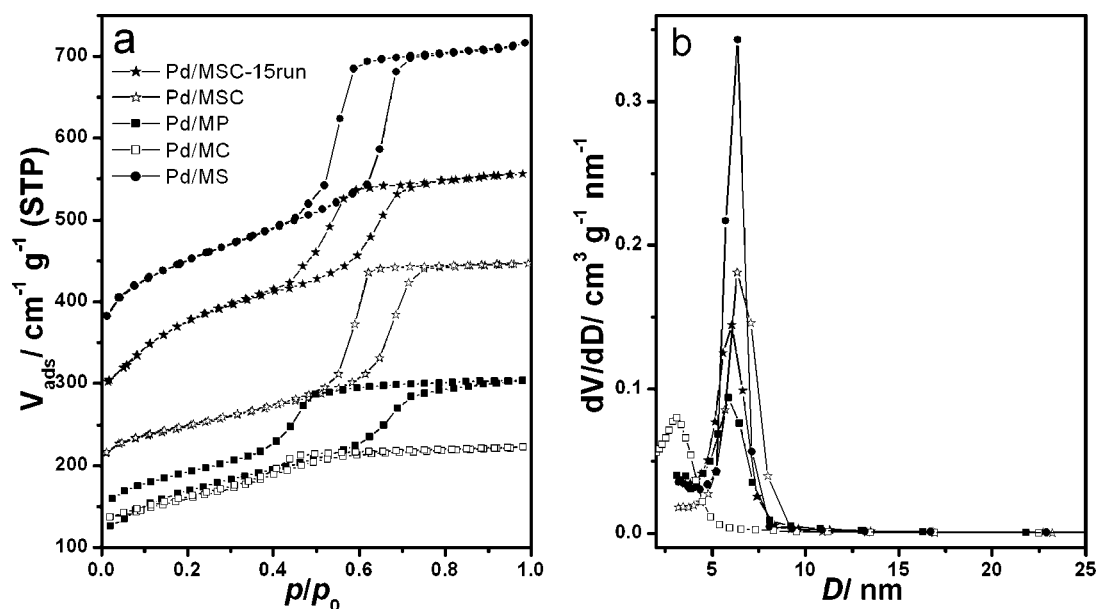


Figure 3. Nitrogen sorption isotherms (a) and pore size distribution curves (b) of the fresh (Pd/MSC, Pd/MP, Pd/MC, and Pd/MS) mesoporous supported palladium catalysts on silica–carbon nanocomposite, polymer, carbon, and silica and the spent Pd/MSC-15run catalyst after 15 catalytic Heck reaction runs. The isotherms (a) for the supported Pd catalysts Pd/MP, Pd/MSC, Pd/MSC-15run, and Pd/MS are offset vertically by 50, 150, 180, and 280 cm^3/g , respectively.

Table 1. Structural and Textual Parameters of the Supports, Fresh Supported Palladium Catalysts after Reduction in Forming Gas, and a Catalyst after 15 Catalytic Runs in the Heck Reaction

sample	a_0 (nm)	S_{BET} (m^2/g)	D_p (nm)	V_i (cm^3/g)
MSC	11.2	413	6.3	0.53
Pd/MSC	10.9	345	6.3	0.46
Pd/MSC-15run ^a	10.9	590	6.0	0.61
MP	14.3	479	6.4	0.44
Pd/MP	13.4	421	5.9	0.39
MC	9.8	682	3.2	0.44
Pd/MC	9.6	523	3.1	0.34
MS	11.1	699	6.3	0.80
Pd/MS	10.5	605	6.3	0.67

^a The Pd/MSC catalyst after 15 runs.

about 21° due to polymeric framework. Several well-resolved peaks at $2\theta = 40.1, 46.5, 68.0$ and 82.1° are observed in fresh

Pd/MP and Pd/MS, assignable to the 111, 200, 220, and 311 reflections of the face-centered cubic (fcc) Pd lattice. The sharp peaks indicate the growth of metallic Pd in these two catalysts after reduction in forming gas. According to the Scherrer formula, the palladium particle size is estimated to be 6.1 and 8.4 nm for Pd/MP and Pd/MS, respectively. The wide-angle XRD reflections of metallic Pd in Pd/MSC and Pd/MC catalysts are broad and indistinguishable due to the overlap by the diffraction peaks of carbon, implying relatively small palladium nanoparticles. XPS spectra (Figure 5) demonstrate that the Pd species in all fresh catalysts (Pd/MSC, Pd/MP, Pd/MC, and Pd/MS after reduction in forming gas) are presented in the metallic

(70) Thomas, A. C. *Photoelectron and Auger Spectroscopy*, 1st ed.; Plenum: New York, 1975; p 352.

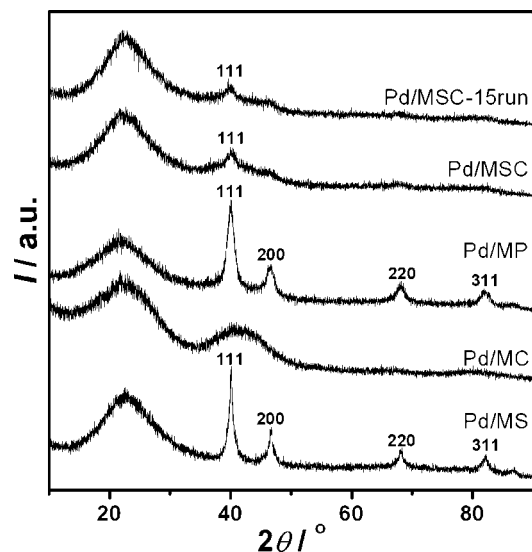


Figure 4. Wide-angle XRD patterns of fresh palladium catalysts supported on mesoporous silica-carbon (MSC), polymer (MP), carbon (MC), and silica (MS) carriers, and a used catalyst supported on mesoporous silica-carbon carrier (Pd/MSC-15run).

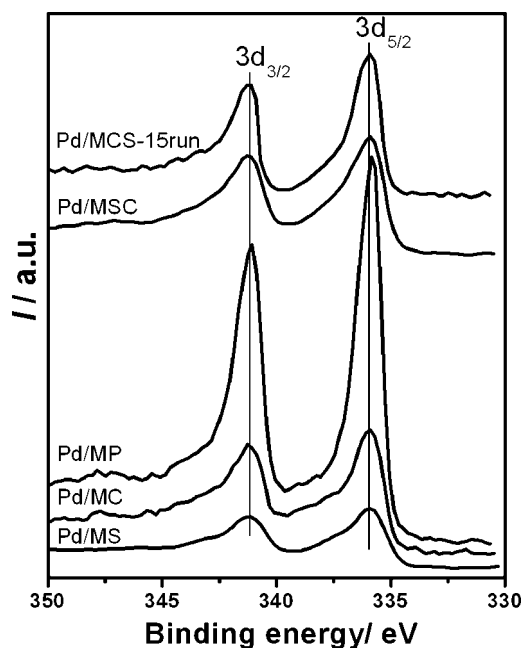


Figure 5. XPS spectra of the fresh and used mesoporous supported palladium catalysts.

state, as evidenced by the two peaks with the binding energy around 340.8 and 335.1 eV in the $3d_{3/2}$ and $3d_{5/2}$ level for Pd(0).⁷⁰

TEM images (Figure 6) show typical stripe-like images for all these fresh catalysts with the 2-D hexagonal mesostructure. However, the dispersion of palladium is distinctly different. Palladium nanoparticles well disperse inside the pores of the Pd/MSC catalyst without obvious aggregation. A STEM-HAADF image (inset Figure 6a) can clearly see the dispersed small metal particles inside mesochannels and no obvious aggregation outside channels. The palladium particle size is about 3 nm, smaller than the pore size for the carrier. This phenomenon demonstrates the accessible metal sites in the pores. Metal nanowires with necklace-like shape grow in the nanochannels of the Pd/MP catalyst. The low-magnification TEM images

show no formation of large Pd particles on the external surface of MP, confirming the formation of metallic nanowires inside the channels. Pd nanowires consisting of connected nanoparticles have the maximum diameter of 6.4 nm and the minimum one at the node of 5.2 nm. On the contrary, no palladium particles or aggregations are clearly observed in the TEM images of the Pd/MC catalyst. However, the EDX analysis reveals the presence of palladium (inset Figure 6c), and the plane scanning (data not shown here) reflects the good dispersion of metallic Pd. These phenomena indicate the small particle size of the metals in Pd/MC. In the Pd/MS catalyst, the dispersion of palladium is not as uniform as that in the Pd/MSC catalyst. Two or three metallic Pd particles aggregate together to form large particles. The observation is in accordance with the XRD results.

The difference in the growth of palladium particles inside the pore channels is possibly related to the nature of the pore wall. Although the capillary force is responsible for the involvement of metallic solution inside the channels, the interaction between solution and pore walls of mesoporous materials is important for impregnation.^{71,72} The growth of necklace-like metal nanowires has been reported by Fukuoka et al.^{73,74} and our group,⁵⁷ by using hybrid silicas with organic groups embedded in the silica framework as carriers. Here we also attribute the formation of Pd nanowires in the mesopores to the interaction of metallic solution with the internal organic polymeric framework of MP. The framework contains plenty of oxygen-containing functional groups such as phenol, benzyl, and carboxyl moieties, which can strongly interact with hydrated palladium ions. The strong interaction between the pore wall and impregnated precursor facilitates the filling of ions along the channels.⁷² During reduction, metallic palladium is formed at the adsorbing site due to the strong adsorption and reducing feature of the polymer, and hence Pd nanowires are coated on the pore surface of MP. Therefore, the low contraction between the pore wall and pore channel may be responsible for the weak intensity of the diffraction peaks in the XRD pattern, rather than the low mesoscopic regularity.

The silanol groups on the surface of MS can also interact with the metallic solution, which favors the mass transfer of palladium solution inside mesochannels. Upon reduction, metal nanoparticles aggregate together in some domains. This phenomenon is similar to that for synthesis of supported metal oxides on mesoporous silica^{71,75} and nanocasting mesostructured metal or metal oxide.⁷⁶ When the nucleation of metal or metal oxides occurs at some domains in the confined mesochannels, the precursors in other areas transfer and nucleate together. Part of the mesochannels in the scaffold is fully filled, and others remain almost empty. Once the scaffold is removed, the obtained metals can replicate the mesostructure with a high loading of precursors. In the present case, the palladium loading is very low. A complete filling of mesochannels and hence the

(71) Liu, Z.; Terasaki, O.; Ohsuna, T.; Hiraga, K.; Shin, H. J.; Ryoo, R. *ChemPhysChem* **2001**, *2*, 229.

(72) Wan, Y.; Yang, H. F.; Zhao, D. Y. *Acc. Chem. Res.* **2006**, *39*, 423.

(73) Fukuoka, A.; Sakamoto, Y.; Guan, S.; Inagaki, S.; Sugimoto, N.; Fukushima, Y.; Hirahara, K.; Iijima, S.; Ichikawa, M. *J. Am. Chem. Soc.* **2001**, *123*, 3373.

(74) Fukuoka, A.; Higuchi, T.; Ohtake, T.; Oshio, T.; Kimura, J.; Sakamoto, Y.; Shimomura, N.; Inagaki, S.; Ichikawa, M. *Chem. Mater.* **2006**, *18*, 337.

(75) Sietsma, J. R. A.; Meeldijk, J. D.; den Breejen, J. P.; Versluijs-Helder, M.; van Dillen, A. J.; de Jongh, P. E.; de Jong, K. P. *Angew. Chem., Int. Ed.* **2007**, *46*, 4547.

(76) Shi, Y. F.; Wan, Y.; Zhang, R. Y.; Zhao, D. Y. *Adv. Funct. Mater.* **2008**, *18*, 2436.

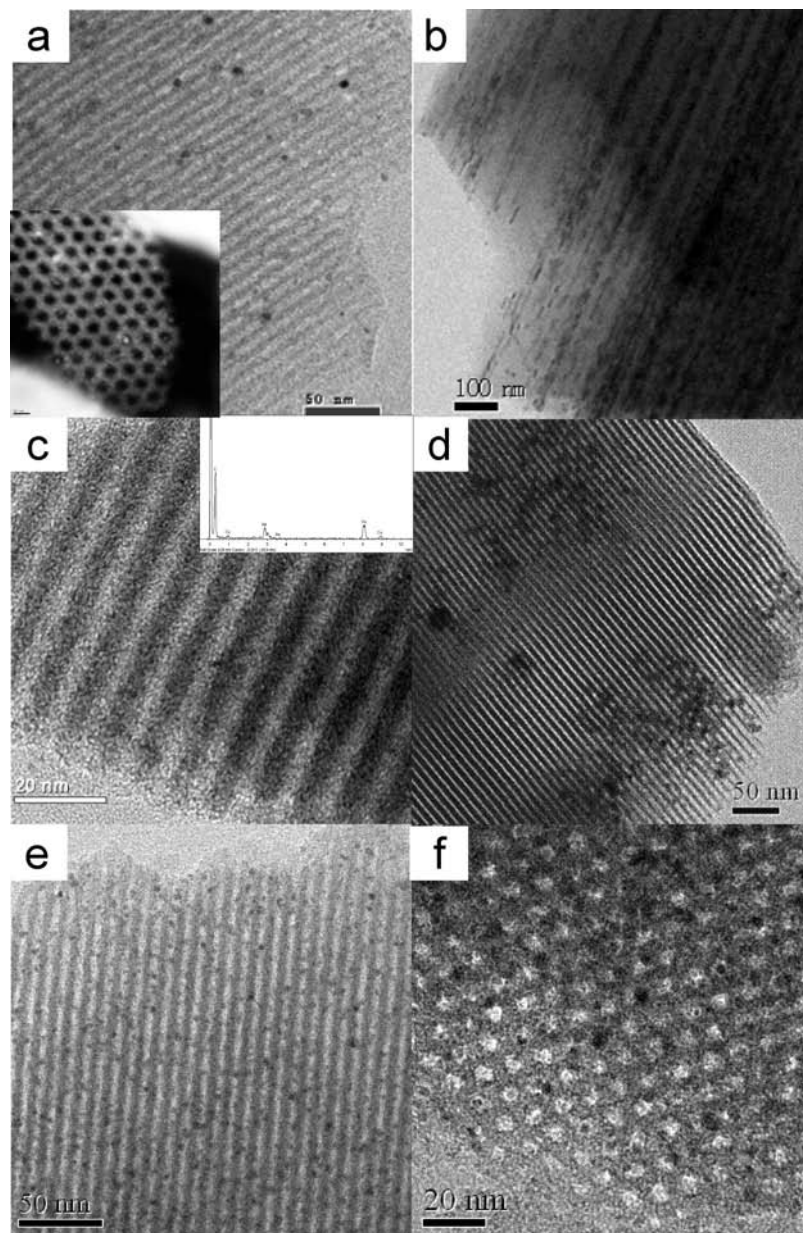


Figure 6. TEM images of the mesoporous supported palladium catalysts: fresh Pd/MSC (a); fresh Pd/MP (b); fresh Pd/MC (c); fresh Pd/MS (d); and used Pd/MSC catalyst after 15 runs (e) and (f). Inset a is the STEM-HAADF image. Inset c is the EDAX pattern.

replication of mesostructure cannot be obtained, but the aggregation of the metal nanoparticles occurs in some regions.

Pure carbon MC carrier has uniform mesopores and plenty of micropores as evidenced by the $V-t$ plot analysis (Supporting Information Figure S3). Almost 57% BET surface area comes from micropores. The generation of these micropores inside the pore walls is mainly due to the release of small molecules during the carbonization of phenolic resins. Metallic solution can uniformly enter the pores due to the well-distributed mesopores of the MC carriers. However, the carbon surface is extremely inert and has weak interaction with palladium ions. So the diffusion of metallic solution into secondary micropores inside the pore walls possibly occurs due to the capillary force. Upon reduction, the Pd nanoparticles are formed in the confined space or at the orifice of these micropores. As a result, no obvious palladium nanoparticles are observed in the TEM images.

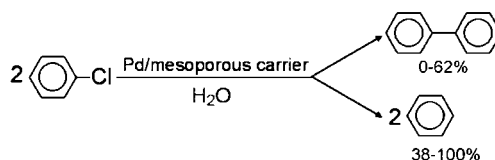
Interestingly, Pd/MSC catalyst has a uniform dispersion of metallic Pd nanoparticles, which can be explained by the hybrid

nature of the carrier. The silica and carbon components uniformly disperse inside the pore walls to construct a continuous framework.¹⁵ Metallic ions may be selectively adsorbed on the surface of silica, which can interact with palladium ions, while the inert, hydrophobic component carbon possibly plays a role to separate them. The confinement of the mesochannel space and the synergistic role from hybrid silica and the carbon nature of the framework lead to the formation of well-dispersed Pd nanoparticles after reduction.

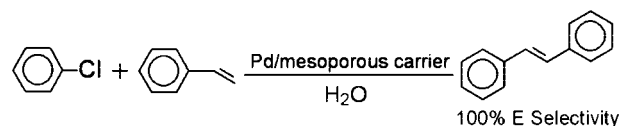
H₂ chemisorption measurements were also used to calculate the specific surface area and size of metallic Pd (Table 2). The specific surface area for the active sites is in the order of Pd/MC > Pd/MSC > Pd/MP > Pd/MS. The corresponding palladium particle sizes are 2.1, 3.5, 8.2, and 10.6 nm, respectively, in good agreement with the XRD and TEM results. To the best of our knowledge, this is the first attempt to study the influence of framework compositions for mesoporous carriers on the metal dispersion. The highly dispersed palladium heterogeneous

Table 2. Metallic Size and the Catalytic Performance for the Heck and Ullmann Coupling Reactions of Chlorobenzene over Supported Palladium Catalysts

Ullmann reaction:



Heck reaction:



sample	d_{Pd}^a (nm)	d_{Pd}^b (nm)	S_{Pd}^c (m ² /g)	catalytic performance					
				Heck reaction ^d		Ullmann reaction ^e			
				100 °C ^f		30 °C ^f		100 °C ^f	
conv. ^g (%)	sel. ^h (%)	conv. ^g (%)	sel. (%)	conv. ^g (%)	sel. (%)				
Pd/MSC		3.5	118	27	100	74	62	100	64
Pd/MP	6.1	8.2	51	9	100	44	0	100	15
Pd/MC		2.1	198	3	100	18	0	100	16
Pd/MS	8.4	10.6	39	<1	100	13	0	20	0

^a Particle size, calculated from the XRD pattern on the basis of the Scherrer formula. ^b Particle size, calculated from the H₂ chemisorption. ^c Specific surface area of active metal, calculated from the H₂ chemisorption. ^d All Heck reactions are carried out in air using 5.0 mmol chlorobenzene, 7.5 mmol styrene, 0.10 g supported palladium catalyst containing 0.047 mmol Pd, 10 mL of water, and 7.5 mmol Na₂CO₃; the reaction time is 24 h. ^e All Ullmann reactions are carried out in air using 10 mmol chlorobenzene, 0.10 g supported palladium catalyst containing 0.047 mmol Pd, 10 mL of water, 21 mmol HCOONa, and 50 mmol KOH; the reaction time is 6 h. ^f Reaction temperature. ^g Conversion of chlorobenzene is determined by GC–mass analysis. ^h Complete *E* selectivity is observed.

catalyst supported on the mesoporous silica–carbon nanocomposite shows potentials in hydrogenation and coupling reactions.

3.3. Coupling Reactions of Aryl Halides in Water. The mesoporous Pd/MSC catalyst was tested on the Heck coupling reaction of chlorobenzene, using styrene as the vinylic substrate. The reactions were carried out using water as the solvent in batch reactors in air and the normal pressure at 100 °C (Table 2). This catalyst exhibits a relatively high conversion (27%) of chlorobenzene and selectivity (100%) to *trans*-stilbene. When bromobenzene is used as a reactant, about 32% reactant converts to the product. These results indicate the ability to activate both aryl chloride and bromide for the Pd/MSC catalyst. The high selectivity for the Heck coupling reaction of aryl borides or aryl iodides was also observed for other Pd heterogeneous catalysts, such as Pd-MCM-41,⁴⁴ Pd/Ph-SiO₂,^{77,78} Pd-SH-SBA-15,⁷⁹ and so on. However, the ability for Pd/MSC is noteworthy in activating chlorobenzene to give a significant yield of the desired products. As far as we know, only a few reports used Pd(0)-based heterogeneous catalysts to catalyze the Heck coupling reaction of chlorobenzene, and all cases adopted organic solvents, such as DMF (Supporting Information Table S1) and sometimes phase-transfer catalyst.^{80–82} For example, 15% yield of *trans*-stilbene can be obtained in the Heck coupling reaction

of chlorobenzene and styrene over Pd(0)-MCM-41 when using DMF as the solvent.⁸¹ To confirm the activation of chlorobenzene, catalytic activity for mesoporous Pd/MSC was also tested on the Ullmann coupling reaction of chlorobenzene in water. Over 74% chlorobenzene can be converted at 30 °C, and the yield for biphenyl is 46%. The dechlorination product benzene is the only detected byproduct. To the best of our knowledge, this is the highest yield of biphenyl from chlorobenzene using water as a solvent on a heterogeneous catalyst at a temperature close to room temperature without any assistance of a phase-transfer catalyst. When the reaction temperature increases to 100 °C, which is normally employed in Ullmann reaction, the conversion of chlorobenzene reaches 100% and the yield of biphenyl reaches 64%. If a cosolvent methanol is added ($V_{CH_3OH}/V_{H_2O} = 1:1$), 90% yield for biphenyl can be achieved. The substituted aryl chlorides, such as 4-chlorophenol, 4-chloroanisole, and 4-chlorotoluene, were also used in the synthesis batch (Table 3). The coupling reaction in water over the Pd/MSC catalyst at a low temperature (30 °C) is highly active. For example, the conversion can reach almost 100%, and the selectivity for the coupling product is 86% for 4,4'-dihydroxy biphenyl, 74% for 4,4'-dimethoxy biphenyl, and 44% for 4,4'-dimethyl biphenyl. The symmetrical biaryls, especially 4,4'-dihydroxy biphenyl, are considered to be prospect chemicals in the market. The only byproduct is dehalogenation product. As a result, the separation of the goal products is easy. The catalytic coupling reactions are of great importance because of the use of water as a clean and environmentally benign solvent and chlorobenzene as the reactant. In addition, compared with our previous results,^{56,57} in which 0.5 g of 6 wt % Pd/organosilica catalyst (6 times higher amount of palladium than this case) was used for the production of biphenyl from

(77) Molnar, A.; Papp, A.; Miklos, K.; Forgo, P. *Chem. Commun.* **2003**, 2626.

(78) Papp, A.; Miklos, K.; Forgo, M.; Molnar, A. *J. Mol. Catal. A* **2005**, 229, 107.

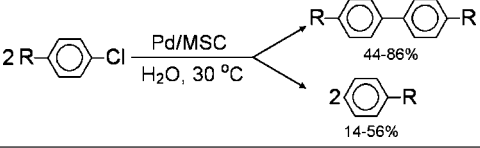
(79) Crudden, C. M.; Sateesh, M.; Lewis, R. *J. Am. Chem. Soc.* **2005**, 127, 10045.

(80) Ding, J. H.; Gin, D. L. *Chem. Mater.* **2000**, 12, 22.

(81) Jana, S.; Dutta, B.; Bera, R.; Koner, S. *Inorg. Chem.* **2008**, 47, 5512.

(82) Prockl, S. S.; Kleist, W.; Gruber, M. A.; Kohler, K. *Angew. Chem., Int. Ed.* **2004**, 43, 1881.

(83) Karimi, B.; Enders, D. *Org. Lett.* **2006**, 8, 1237.

Table 3. Catalytic Performance in Coupling Reaction for Substituted Chlorobenzene over the Pd/MSC Catalyst^a


reactant	R	conv. (%)	sel. (%)
1	OH	>99	86
2	CH ₃	>99	44
3	OCH ₃	>99	74

^a All Ullmann reactions are carried out in air using 10 mmol substituted aryl chloride, 0.10 g supported palladium catalyst containing 0.047 mmol Pd, 10 mL of water, 21 mmol HCOONa, and 50 mmol KOH; the reaction temperature is 30 °C, and the reaction time is 6 h.

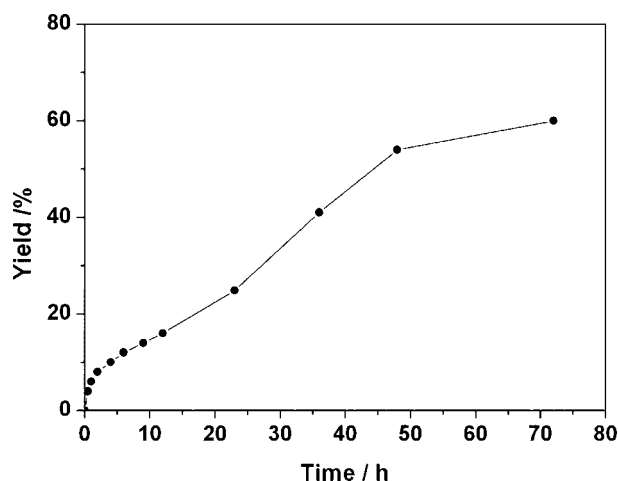


Figure 7. Time conversion plot for the Heck reaction of chlorobenzene (1.1 g, 10 mmol), styrene (1.56 g, 15 mmol), and sodium carbonate (1.6 g, 15 mmol) in water (20 mL) at 100 °C in the presence of Pd/MSC (0.20 g) as a catalyst.

bromobenzene and iodobenzene, the present process is more efficient and economic.

To further improve the Heck coupling yield, several parameters were adjusted, such as the prolongation of the reaction time and the increase of the catalyst/reactant ratio. Figure 7 shows the time conversion using the Pd/MSC catalyst. It is clear that, with the prolongation of the reaction time, the coupling yield increases. A yield close to 60% for *trans*-stilbene can be achieved when the reaction time is 72 h. Therefore, the catalyst deactivation does not occur in the reaction. We also increased the catalyst amount or reduced the reactant amount. The increase of the catalyst amount from 0.1 to 0.8 g results in a dramatic but not linear increase for the catalytic activity. The yield of *trans*-stilbene can increase to 55% with addition of 0.8 g of catalyst (reaction time of 24 h).

The liquid phase of the reaction mixture is collected by hot filtration after each reaction to test if palladium is leaching from the solid catalyst during reaction.^{67,68,83} Hot filtration is considered to be an easy and facile means to determine the Pd leaching from the heterogeneous catalyst. ICP-AES analysis confirms an extremely low amount of Pd (less than 0.2%) in the reaction mixture. Even if a long time reaction (72 h) was carried out or a large amount of the catalyst (0.8 g) was added, a low Pd leaching amount (less than 0.2%) is detected after reaction for both cases. In a separated test, the Heck reaction

mixture is hot filtered to collect the liquid phase after 2 h stirring. The conversion of chlorobenzene is 8%. The ICP-AES analysis results from the liquid phases show that a very low amount of Pd (<0.2%) is found. Simultaneously, negligible change for the yield of *trans*-stilbene after a further 22 h reaction is observed (<3%, less than the experimental error). These results clearly suggest that Pd leaching and the catalytic activity by the leaching Pd ions could be approximately excluded in the present coupling reactions. Therefore, the reactions approximately proceed in heterogeneous conditions, where the reactant selectively adsorbs on active centers and then converts to the product. The high activity of Pd/MSC catalyst can be assigned to accessible, small, well-distributed metallic Pd nanoparticles inside the large size and hybrid mesochannels. The metal nanoparticles show a high activity in activating chlorobenzene, and the relatively hydrophobic surface (contribution from the carbon component) and the large mesopore size of silica–carbon nanocomposite facilitate the selective adsorption of substrate in water and mass transfer inside the pores.

3.4. Comparison of Catalytic Performance on Mesoporous Carriers with Different Compositions. The catalytic performance for supported palladium catalysts with different pore wall surface properties and metallic Pd sizes was also tested (Table 2). The mesoporous polymer-based catalyst Pd/MP displays a conversion of 9% for chlorobenzene in Heck reaction at 100 °C. The polymeric framework contains aromatic rings, which have the ability to selectively adsorb chlorobenzene. However, the activation for the aryl chloride on large palladium nanowires of Pd/MP is possibly weaker, leading to an activity lower than that on small Pd nanoparticles of Pd/MSC. A conversion of 44% for chlorobenzene is detected over Pd/MP in Ullmann coupling reaction at 30 °C, but with a negligible formation of biphenyl. The conversion is also lower than that on Pd/MSC. Benzene is the only product, even when the reaction temperature increases to 70 °C. Only 15% biphenyl can be detected on this catalyst at 100 °C; at the same time, the conversion reaches 100%. The low selectivity may be related to the steric restriction in the mesopores which are occupied by palladium nanowires. Benzene with a small molecular size instead of biphenyl is easily formed.

The active specific surface area for Pd/MC is high, and the metallic particle size is small; however, the catalyst shows a low coupling performance, such as 3% conversion in Heck coupling reaction at 100 °C and 18% conversion in Ullmann reaction at 30 °C. This phenomenon can be explained by the fact that small palladium particles locate in the micropores of MC, as shown in TEM images, and the accessibility for these sites by chlorobenzene is low.

When the palladium particles are supported by a pure mesoporous silicate carrier, the catalyst shows an extremely low conversion of chlorobenzene (<1% for Heck reaction and 20% for Ullmann reaction at 100 °C). This behavior may be related to the large metal particle size and hydrophilic nature of the silicate pore walls. The aggregation of Pd particles is responsible for the low activity in activating chlorobenzene. On the other hand, it is difficult for chlorobenzene and styrene to be attracted inside the pores of mesoporous silica in the presence of a large amount of water due to the hydrophilic surface.^{56,57} The low concentration of reactants in the pores restricts the reaction.

3.5. Recycling of the Catalyst. For the recycling study, Heck reaction was performed with chlorobenzene and styrene, maintaining the same reaction conditions as described above except using the recovered catalyst. Up to 21 successive runs

Table 4. Catalytic Performance of Pd/MSC Catalyst and the Recovered Pd/MSC Catalyst in Successive Heck Coupling Runs^a

entry	catalyst amount (g)	catalytic run	conv. (%)	sel. (%)	yield (%)
1	0.2	1	30	100	30
2	0.5	1	46	100	46
3	0.8	1	55	100	55
4	0.1	2	24	100	24
5	0.1	3	23	100	23
6	0.1	5	25	100	25
7	0.1	10	24	100	24
8	0.1	15	26	100	26
9	0.1	21	25	100	25
10	0.2	2 ^b	27	100	27
11	0.5	2 ^b	48	100	48

^a Heck reactions are carried out in air using 5.0 mmol chlorobenzene, 7.5 mmol styrene, 10 mL of water, and 7.5 mmol Na₂CO₃. The reaction time is 24, and the reaction temperature is 100 °C. In the first run, 0.10–1 g of fresh supported palladium catalyst containing 0.047 mmol Pd is added. After reaction, the catalyst is recovered by cold centrifugation, washing and drying and used in the successive runs. In the last run, hot filtration is adopted to separate the catalyst and analyze the Pd leaching. ^b Hot filtration is adopted in the first catalytic run to recover the catalyst.

were tested. The catalytic performance of recovered Pd/MSC (separated by cold filtration) is almost the same for C–C coupling reaction in each run (Table 4), indicating that the catalyst is very stable and can be recycled more than 20 times. The Pd content, after 21 catalytic runs and separation by hot filtration, is approximate 4.9 wt %, implying the negligible metal leaching during the repeated reactions. Hot filtration was also adopted to separate catalyst solid and liquid phase products. For example, the catalysts in the reactions with the initial adding amount of 0.2 or 0.5 g were separated by hot filtration. The recovered catalysts exhibit the catalytic activity with negligible change in comparison to the fresh catalysts. These phenomena further indicate the stability of the catalyst and heterogeneous catalysis.

The XRD pattern, N₂ sorption isotherms, and XPS spectrum for the catalyst after 15 runs are shown in Figures 2b, 3, and 5. The results clearly show that the ordered 2-D mesostructure, high surface area, uniform mesopores, and metallic Pd(0) active sites can be retained after reactions. The wide-angle XRD pattern (Figure 4) and TEM images (Figure 6e,f) reveal the high dispersion of Pd without distinct aggregation of large particles after 15 reactions under 100 °C. These phenomena demonstrate that the heterogeneous catalyst is stable. The reaction conditions have a minor effect on the catalyst structure. Therefore, the silica–carbon framework can support the palladium nanoparticles and restrict the leaching and aggregation of metal. The

reusability of the Pd/MSC catalyst offers a good opportunity for practical applications in coupling reaction and hydrogenation.

4. Conclusions

Heterogeneous palladium catalysts have been supported on ordered mesoporous hybrid silica–carbon materials, which are synthesized by a triblock copolymer templating approach. The novel Pd catalyst exhibits a high yield of *trans*-stilbene of ~60% at 100 °C in Heck coupling of chlorobenzene and styrene and of 46% for biphenyl at 30 °C in Ullmann coupling of chlorobenzene, using water as a solvent on a heterogeneous catalyst without any assistance of a phase-transfer catalyst. When substituted aryl chlorides (such as –OH, –OCH₃, and –CH₃) are involved in the system, the yield of substituted biphenyl can reach 44–86% at a low temperature of 30 °C. The heterogeneous Pd/MSC catalyst shows great advantage in activating aryl chlorides and using water as a clean solvent. The high catalytic performance can be attributed to the hybrid pore surface constituted by continuous and interpenetrated silica and carbon components, large pore size, uniform dispersion of Pd, and relatively small metal particle size. In addition, this heterogeneous catalyst is stable, which shows negligible metal leaching, and can be reused more than 20 times. Mesoporous carriers with different framework compositions, such as polymer, carbon, and silica, are also synthesized on the basis of a self-assembling route. The pore wall composition shows great influence on the metal size and dispersion and hence catalytic performance. The conversion of aryl chloride and selectivity to the goal product over Pd/MP, Pd/MC, and Pd/MS are lower than those on Pd/MSC. The use of a mesoporous hybrid silica–carbon carrier provides a mild, economic, and green route for the C–C coupling reactions.

Acknowledgment. This work was supported by NSF of China (20873086 and 20521140450), Shanghai Sci. & Tech. and Education Committee (07QH14011, 07SG49, 07DZ22303, and 08JC1417100), and the program for New Century Excellent Talents in Universities (NCET-07-0560). The Knut and Alice Wallenberg Foundation is acknowledged for the JEM 2100F microscope. We would like to thank Prof. H. X. Li for helpful discussions.

Supporting Information Available: Heck coupling reaction of chlorobenzene and styrene over a variety of heterogeneous Pd catalysts; TG analyses, N₂ sorption isotherms, pore size distribution curves, and *V*–*t* plots of mesoporous carriers. This material is available free of charge via the Internet at <http://pubs.acs.org>.

JA808481G